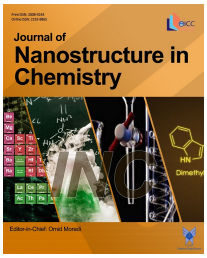

Volume 15, Issue 4, 152515 (1-13)

Journal of Nanostructure in Chemistry (JNSC)

https://doi.org/10.57647/jnsc.2025.1504.15

Pretreatment-Free Rapid Detection of Tiamulin in Egg and Milk Samples using Gold Nanoparticles Based on Positive List System Regulations

Munirah Alhammadi[1], Sonam Sonwal[1], Soobin Han[1], Hanseung Kim[1], Dong-Hwan Kim[2,*], Mi-Hwa Oh[3,*], Yun Suk Huh[1,*]

[1]*Department of Biological Sciences and Bioengineering, Inha University, Incheon, Republic of Korea.*
[2]*School of Chemical Engineering, Sungkyunkwan University, Suwon 16419, Republic of Korea.*
[3]*National Institute of Animal Science, Rural Development Administration, Wanju, South Korea.*

[*]**Corresponding authors:** dhkim1@skku.edu, moh@korea.kr, yunsuk.huh@inha.ac.kr

Original Research

Received:
27 May 2025
Revised:
12 August 2025
Accepted:
31 August 2025
Published online:
31 August 2025

Abstract:

Tiamulin (TML) antibiotic residues in animal products could pose potential health hazards to consumers. South Korea set the positive list system regulations, where the maximum residue limits of TML in poultry eggs should not exceed 1000 ng/mL. Therefore, we developed a simple and pretreatment-free lateral flow immunoassay based on a highly specific TML antibody conjugated with gold nanoparticles for qualitative and semi-quantitative analysis of TML. The optimized sensor showed a visual limit of detection of 15 ng/mL for both milk- and egg-spiked samples, with a cut-off value of 100 ng/mL and 180 ng/mL for milk and egg, respectively. The assay demonstrated high recovery in both milk and egg matrices with relative standard deviation values below 12%, confirming its suitability for rapid and reliable determination of TML in complex food samples. As both sample types required no pretreatment and provided visible results within 10 minutes, the sensor is simple, user-friendly, and highly tolerant to matrix interferences. Moreover, it exhibited specific selectivity toward TML, supporting its potential as a promising detection platform for monitoring TML in animal products.

Keywords: Immunochromatographic assay; On-site detection; Antibody; Tiamulin; Pretreatment-free; Gold nanoparticles

Cite this article: Alhammadi, M., Sonwal, S., Han, S., Kim, H., Kim, D.-H., Oh, M.-H., Huh, Y.S. Pretreatment-Free Rapid Detection of Tiamulin in Egg and Milk Samples using Gold Nanoparticles Based on Positive List System Regulations. *J Nanostruct Chem* **15**(4), 152515 (2025).

1. Introduction

Tiamulin (TML) is a pleuromutilin veterinary antibiotic that is active against Gram-positive bacteria, such as streptococci and staphylococci, spirochetes such as Brachyspira spp., and various mycoplasmata [1]. TML is also used as a feed additive to encourage growth in cattle and swine [2]. However, when veterinary drugs, including TML, are administered inappropriately or excessively in animals, this can lead to drug residues in edible animal tissues [3]. TML residues in animal-derived foods can lead to many adverse biological effects and allergic reactions in consumers [4]. In South Korea, the usage of TML as a veterinary antibiotic is continuously increasing, specifically in pigs, cows, and chickens [5]. To ensure public health safety when consuming animal dairy and meat products, the Ministry of Food and Drug Safety (MFDS) in South Korea has set the positive list system regulations. According to MDFS, the maximum residue limits (MRLs) of TML in poultry eggs should not exceed 1000 ng/mL.

The detection of TML has been done through conventional techniques, including ultra-high-performance liquid chromatography coupled with tandem mass spectrometry (UHPLC-MS/MS) [1, 4, 6, 7], electrochemical immunosensors [8], and indirect competitive fluorescent immunosorbent assays (icFLISA) [9, 10]. These techniques have low detection limits and high accuracy, but they require trained

and skilled personnel to operate and analyze. Furthermore, these techniques require several steps of sample pretreatment such as solid-phase microextraction and dispersive liquid–liquid microextraction resulting in complex and lengthy analysis times [11, 12]. In contrast, lateral flow immunoassays (LFIA) have emerged as promising alternatives for rapid, cost-effective, and field-applicable detection techniques for veterinary drug residues. Recent advancements in nanomaterial-based LFIAs, particularly those using gold nanoparticles (AuNPs), have significantly contributed to improving sensitivity and visual readability [13–15]. Despite these advances, several challenges are there, such as achieving high selectivity and sensitivity in complex food matrices including animal-derived foods, eliminating the need for complex pretreatment steps, and ensuring that detection limits align with regulatory requirements [16]. Despite the widespread use of TML in veterinary medicine, only two studies have previously described LFIAs for its detection, highlighting the limited research attention given to this target in rapid on-site screening formats [17, 18]. Reported LFIA for TML detection have several limitations including lower antibody specificity due to simultaneous antibiotic detection approach, using LFIA wet method which could cause stability issues and batch-to-batch variability, and complex real sample pretreatment steps; these factors collectively compromise analytical sensitivity and restrict the method's applicability in rapid, field-based screening.

To address these issues, we developed a pretreatment-free LFIA based on AuNP-labeled TML antibodies for specific detection of TML residues in egg and milk samples. This work aims to deliver a user-friendly, rapid screening tool with high sensitivity and selectivity that aligns with the positive list system criteria while offering high tolerance for matrix complexity.

2. Materials and methods

2.1 Reagents and instruments

TML, polyvinyl alcohol, gold (III) chloride trihydrate ($\geq$ 99.9), bovine serum albumin (BSA), tween 20, valnemulin (VAL), tylosin (TYL), ampicillin (AMP), chloramphenicol (CPL), tetracycline (TET), ractopamine (RAC), trisodium citrate dihydrate, and creatine were purchased from Sigma–Aldrich, USA. BSA-TML (coating antigen) and TML-Ab (mouse anti-tiamulin monoclonal antibody) were obtained from Creative Diagnostics, USA. Detailed specifications of the antibodies used in this study are provided in supplementary information (Supplementary Table 1). LFIA composites, including nitrocellulose membrane (Membrane thickness: 95 – 135 µm, pore size: 15 µm), absorbent pad, conjugate pad, sample pad, and backing card, were obtained from Bore Da Biotech, South Korea. Detailed specifications of the nitrocellulose membrane used in this study are provided in supplementary information (Supplementary Table 2). Milk and egg products used for spiked samples were purchased from a local market in Incheon (South Korea). All other auxiliary reagents were of higher chemical or analytical grades.

The HAG rotator (FINEPCR, South Korea) was utilized for sample rotation. Deionized water was obtained from Molsheim Millipore, France. VS-15000CFNII centrifuge (Vision Scientific, South Korea) was used for sample centrifugation. To cut LFIA sheets, an AR-100CG cutter (THiRA-ARTROBO, South Korea) was used. JEM-2100F field-emission transmission electron microscopy (FE-TEM) (JEOL, Japan) and high-resolution X-ray diffractometer (XRD) (Rigaku, Japan) were utilized for AuNPs characterization. A V-770 UV-Visible/NIR spectrophotometer (UV-Vis) (TS Science, South Korea) was utilized for measuring absorbance peaks. Dynamic Light Scattering (DLS) and zeta potential were measured using zetasizer pro (Malvern Panalytical, England).

2.2 Gold nanoparticles synthesis protocol

The synthesis of AuNPs was done using Turkevich as previously described with some modifications [19]. Briefly, 300 mL of deionized water in a reaction vessel is heated to 380 °C and stirred at the speed of 200 rpm. Upon water boiling, 700 µL of 10% $HAuCl_4 \cdot 3H_2O$ is added, and after 2 minutes, 4.6 mL of 1% trisodium citrate dihydrate solution is added and heated for 2 minutes. The solution color changing from yellow to red wine can be observed. Using potassium carbonate (K_2CO_3), the AuNPs solution pH was set to 9.0. The AuNPs solution was kept in the fridge for further use.

2.3 Gold nanoparticle-antibody probe preparation

The binding of TML-Ab to AuNPs was prepared as previously described in our research paper [20] with small modification. Briefly, the prepared AuNPs colloid solution is mixed with 2 µg/mL TML-Ab and reacted at room temperature in a rotator for 30 minutes at 30 rpm speed. Removal of non-bound antibodies was done by centrifuging the AuNPs-TML-Ab solution for 15 minutes at 6000 rpm and 4 °C. Through this step, the TML-Ab is adsorbed to the surface of AuNPs through electrostatic attraction. After removing the supernatant, the pellet was resuspended with 1% of BSA blocking reagent to block non-specific binding and 10 mM phosphate buffer (PB). The rotating, centrifugation, and blocking procedures were performed again twice to ensure the removal of impurities and non-bounded antibody. The concentration of the AuNP-TML-Ab conjugate was standardized by adjusting the optical density to 8 at 527 nm to ensure reproducibility of the LFIA performance. At the final step, the pellet combining of TML-Ab conjugated with AuNPs was again resuspended with 5% sucrose, PB, and 1% BSA.

2.4 Fabrication of the LFIA strip and the detection procedure

Strips used for LFIA contain four main overlapping parts, including a conjugation pad, sample application pad, absorbent pad, and nitrocellulose membrane, assembled on a backing card (Fig. 1 (a)) [21]. The fabrication procedure of the LFIA strips was done as previously described [20]. Briefly, the conjugation pad was pre-treated with tween 20 and polyvinyl alcohol for prevention of non-specific binding. The solution containing AuNPs-TML-Ab was dropped on the conjugate pad and kept for drying overnight. When dropping the test solution onto the sample pad, the solution

will flow through the strip by capillary force, passing the conjugate pad, the nitrocellulose membrane, which contains immobilized capture molecules on the test and control lines, and finally to the absorbent pad [22]. The final assembled LFIA sheets were cut into 4.0 mm width strips and kept in a desiccator for further use.

For testing, 150 µL of standard solution made of different concentrations of TML mixed with running buffer is dropped over the sample pad on the test strip, and the results can be observed within 10 minutes, as shown in Fig. 1 (a). When testing a positive sample, the target analyte will flow from the sample pad through the test strip, binding to the capture probe (AuNP-TML-Ab) on the conjugate pad, then passing the test line, which contains an immobilized BSA-TML (1.0 mg/mL), and control line, which contains goat anti-mouse IgG (1.0 mg/mL), to the absorbent pad, resulting in the disappearance of the test line (Fig. 1 (a)). In the case of a negative sample, the AuNP-TML-Ab probe will migrate in the test strip, binding to the BSA-TML coating antigen on the test line, resulting in the observation of red color on the test strip.

2.5 Sensitivity of LFIA Strip to tiamulin in standard and spiked samples

The developed test strip's capability of sensing TML was investigated by testing various concentrations of TML (0, 1, 5, 10, 15, 20, 50, 70, 80, 100, and 1000 ng/mL) in standard solution. After 10 minutes of adding 150 µL of sample solution to the test strips, two lines demonstrating the test and control line can be observed. The results obtained were photographed, processed, and analyzed further using ImageJ software. The specificity of the sensor was evaluated by testing the cross-reactivity with TML analogs TYL, VAL, and other possible interference molecules such as RAC, creatine, AMP, TET, and CPL.

For real-sample evaluation, fresh chicken egg and cow milk samples were obtained from local markets and confirmed to be free of TML by initial screening using the developed assay. To evaluate the sensor's performance in complex matrices, these samples were spiked with various concentrations of TML and analyzed under the same assay conditions. Relative standard deviation (RSD) values were calculated for each concentration to assess assay precision in accordance with standard analytical validation practices. Recovery (%) was determined by comparing the measured concentration in each spiked sample to the known spiked concentration and multiplying by 100. Also, the limit of quantification (LOQ) was defined as the lowest analyte concentration that could be quantified with acceptable accuracy ($80-120\%$ recovery) and precision (RSD $\leq 15\%$) based on replicate spiked sample analyses [23]. All values are reported as mean $\pm$ RSD from triplicate measurements. The experimental workflow is summarized in Fig. 1 (b), from AuNPs synthesis and antibody–AuNP conjugation to LFIA assembly, optimization, data analysis, and pretreatment-free real sample testing, followed by performance evaluation.

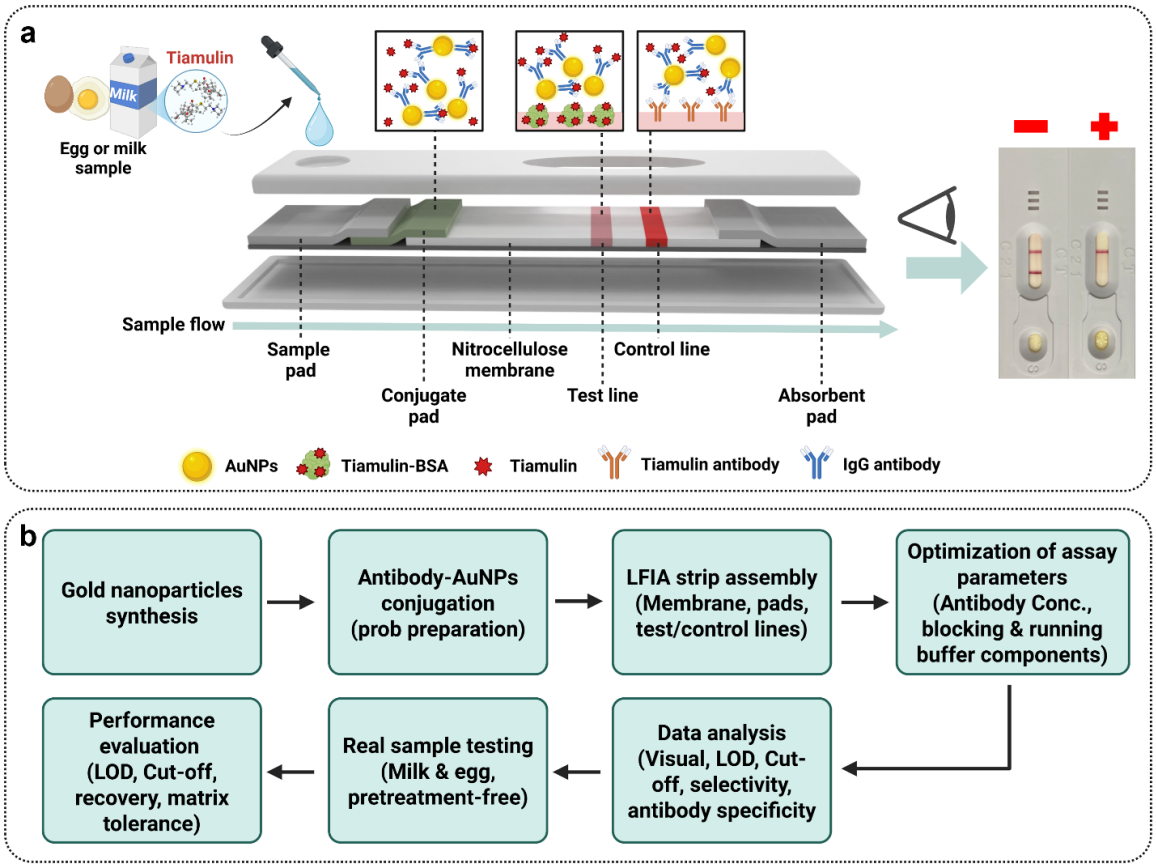

Figure 1. Overview of the developed pretreatment-free LFIA for TML detection. (a) Working principle of LFIA technique and its components. (b) Experimental workflow for LFIA development and evaluation, from nanoparticle synthesis to pretreatment-free real sample testing and data analysis.

3. Results and discussion

3.1 Gold nanoparticles-antibody probe optimization

By utilizing the Turkevich method, the size of AuNP can be controlled by varying the ratios of gold to reducing agent. In this study, AuNPs with a size of $30-40$ nm were used as the optimal size. Fig. 2 (a) depicts the gold colloid UV-Vis absorbance peak at 525.2 nm. The average number of AuNPs was calculated to be $\approx 1.34 \times 10^{12}$ nanoparticles/mL. Fig. 2 (b) shows the histogram graph of AuNPs size distribution with an average diameter of 41.9 nm $\pm$ 4.29. The crystalline structure of the synthesized AuNPs was confirmed by XRD. As shown in Fig. 2 (c), the diffraction pattern exhibits characteristic peaks at 2θ values of approximately 38.2°, 44.4°, 64.8°, and 77.6°, corresponding to the (111), (200), (220), and (311) crystallographic planes of face-centered cubic (fcc) gold (JCPDS No. 04-0784). The strong reflection at $\sim 38.2°$ (111) is the most intense, indicating preferential orientation along this plane, which is commonly observed in colloidal gold nanoparticles. The absence of additional diffraction peaks indicates high phase purity without detectable impurities. The relatively broad peak shapes also reflect the nanocrystalline nature of the AuNPs. These results confirm that the synthesized particles possess the expected fcc structure of metallic gold [24, 25]. In addition, the morphology and crystallinity of the synthesized AuNPs were investigated by FE-TEM. As shown in Fig. 2 (d) and (e), the nanoparticles exhibited a uniform spherical morphology. The selected area electron diffraction (SAED) pattern displayed well-defined diffraction rings corresponding to the fcc structure of gold (Fig. 2 (f)). Elemental mapping confirmed the presence and homogeneous distribution of C, O, and Au (Fig. 2 (g-i)), while the corresponding energy dispersive spectroscopy (EDS) spectrum showed intense peaks for Au along with minor contributions from C and O, consistent with citrate-capped AuNPs (Fig. 2 (j)). These results verify the successful synthesis of crystalline gold nanoparticles with high purity.

The conjugation of TML-Ab to AuNPs was confirmed by both UV–Vis spectroscopy and zeta potential measurements. Compared with bare AuNPs, the presence of TML-Ab in the probe induced a slight red shift in the surface plasmon resonance band (Fig. 3 (a)), consistent with surface modification of AuNPs. In addition, zeta potential analysis revealed a reduction in surface charge from -39.18 mV for citrate-AuNPs to -15.7 mV after antibody attachment (Fig. 3 (b) and c). The observed spectral shift and decrease in negative potential together provide strong evidence of successful AuNP–TML-Ab conjugation [26–28].

The optimal TML-Ab concentration for the LFIA procedure was determined by testing antibody concentrations of 0, 1, 2, 3, 4, and 5 µg/mL. Samples containing TML at 0, 10, 100, and 1000 ng/mL were applied to test strips prepared with different antibody concentrations (Fig. 3 (d)). Strips without TML-Ab showed no visible coloration, whereas strips containing TML-Ab displayed increasing test line and control line color intensity as the antibody concentration increased from 1 to 5 µg/mL. Since this LFIA system operates in a competitive format, at 0 ng/mL TML the test line appeared dark red, and as the TML concentration increased ($10-1000$ ng/mL), the test line intensity decreased proportionally until disappearing at the cut-off value. Here, the cut-off value is defined as the TML concentration at which the test line disappears, and the visual limit of detection (vLOD) is defined as the concentration at which the test line intensity is visibly distinguishable from the negative control (0 ng/mL) [29]. An antibody concentration of 2 µg/mL was selected as optimal, as it provided results that were clearly distinguishable by the naked eye and offered higher sensitivity toward TML compared to higher antibody

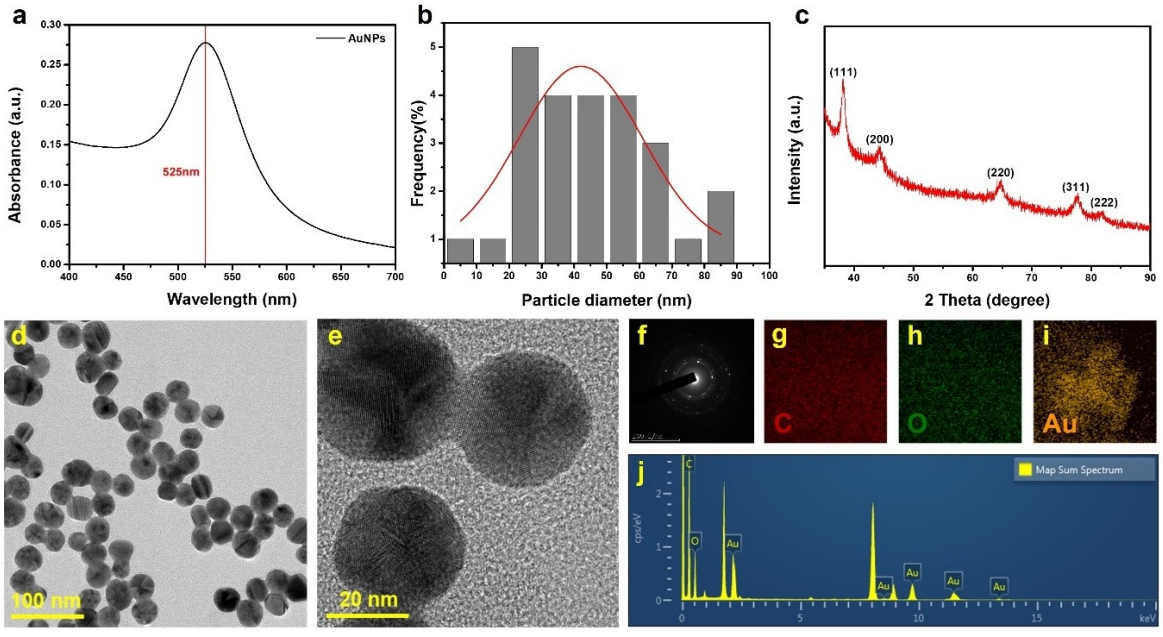

Figure 2. Characterization of the synthesized AuNPs. (a) UV-Vis absorption spectra of the gold colloid. (b) Size distribution histogram of AuNPs. (c) XRD pattern of AuNPs showing peaks of the fcc gold structure (JCPDS No. 04-0784). (d-e) FE-TEM images of synthesized AuNPs. (f) SAED pattern image of AuNPs and (g-j) the corresponding EDS mapping images of carbon, oxygen, and gold.

concentrations, where sensitivity declined. To ensure reproducibility and stability of the probe, the AuNP–TML-Ab conjugate concentration was standardized by adjusting the optical density to 8 at 527 nm prior to LFIA assembly.

3.2 LFIA strip optimization

Optimization of the main parameters in the LFIA sensing procedure was conducted to achieve a highly sensitive and specific LFIA system for TML detection. The optimization procedure was performed referring to our previously published research [20, 30]. Briefly, blocking buffer type (20 mM borate buffer, 10 mM phosphate-buffered saline (PBS), and 10 mM PB), blocking buffer pH (7, 8, or 9), and running buffer components including NaCl and tween 20 were optimized to attain the highest sensitivity. First, the blocking buffer, which is used throughout the AuNP-anti-TML conjugation procedure, was chosen to be PB since it showed the highest sensitivity, as illustrated in Supplementary Fig. 1. Next, we determined the optimized blocking buffer pH by testing various pH of PB, and PB of pH 9.0 was selected because of high sensitivity and clear background compared to other pH values (Supplementary Fig. 2). Moreover, when preparing testing samples, the components included in the running buffer have a significant effect on the sensing results. After testing NaCl with concentrations of 0, 18.75, 37.5, 75, 150, and 300 mM, 150 mM resulted in the best condition for determining TML with good test line color intensity and distribution, as shown in Supplementary Fig. 3. Lastly, tween 20 optimized condition was chosen based on which concentration provided the best solution flow throughout the test strip with the least background effect, and 5% was selected as the optimal condition (Supplementary Fig. 4).

3.3 Sensitivity and specificity of LFIA strips to tiamulin

As demonstrated in Fig. 4, the final optimized LFIA test strips were used to detect TML in standard solution at various concentrations of 0, 1, 5, 10, 15, 20, 22, or 100 ng/mL to determine the developed LFIA sensitivity. In Fig. 4 (a), when TML concentration increases in the sample, the test line slowly starts disappearing until reaching the cut-off

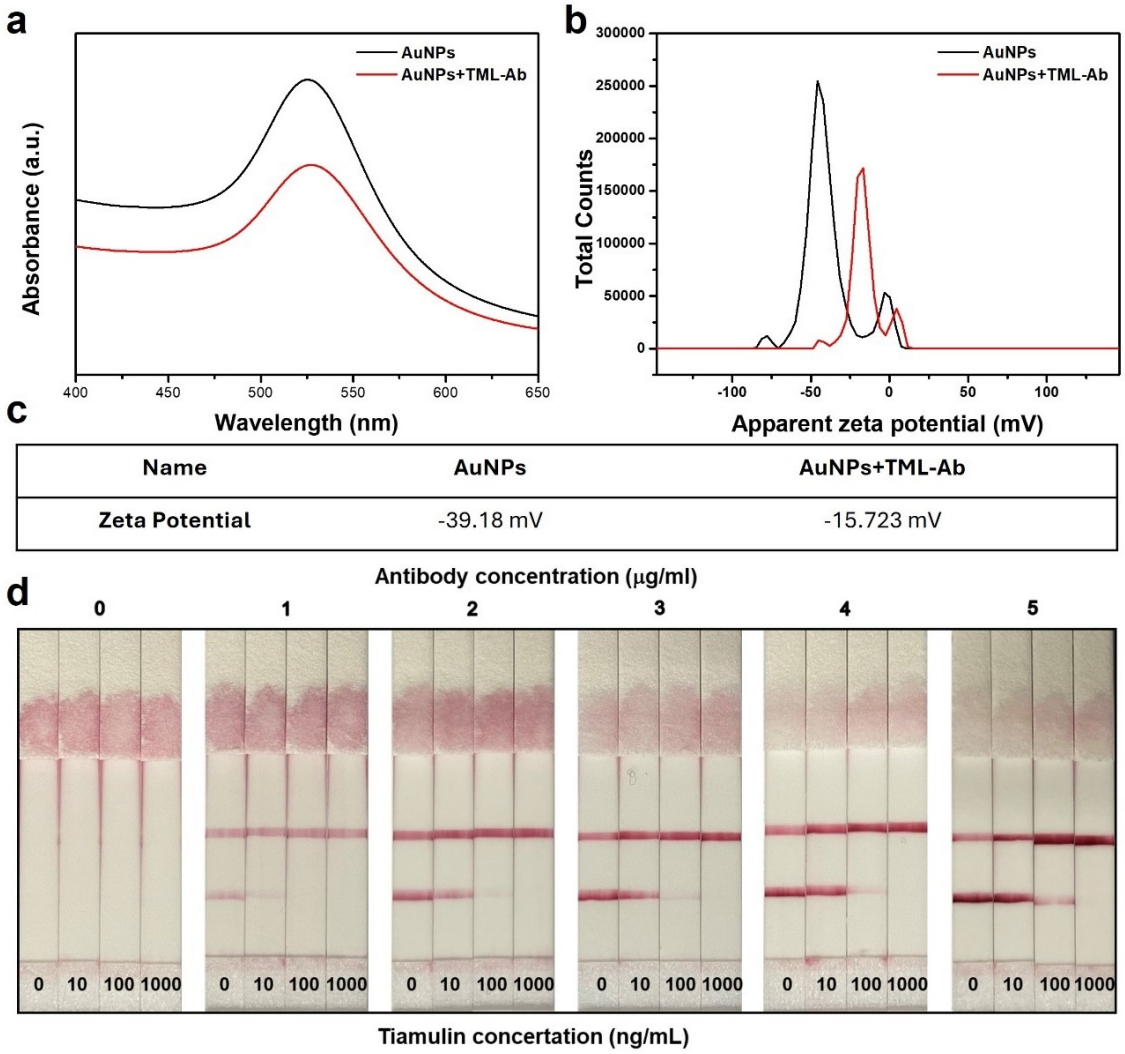

Figure 3. Characterization of AuNP-TML-Ab conjugates and optimization of antibody concentration for LFIA. (a) UV-Vis absorption spectra of bare AuNPs and AuNPs-TML-Ab prob. (b-c) Zeta potential of bare AuNPs and TML-Ab-conjugated AuNPs. (d) Optimization of the LFIA for TML determination. Effect of various concentrations (0, 1, 2, 3, or 4 μg/mL) of TML-Ab on LFIA strip results. The TML sample concentrations used were 0, 10, 100, 1000 ng/mL.

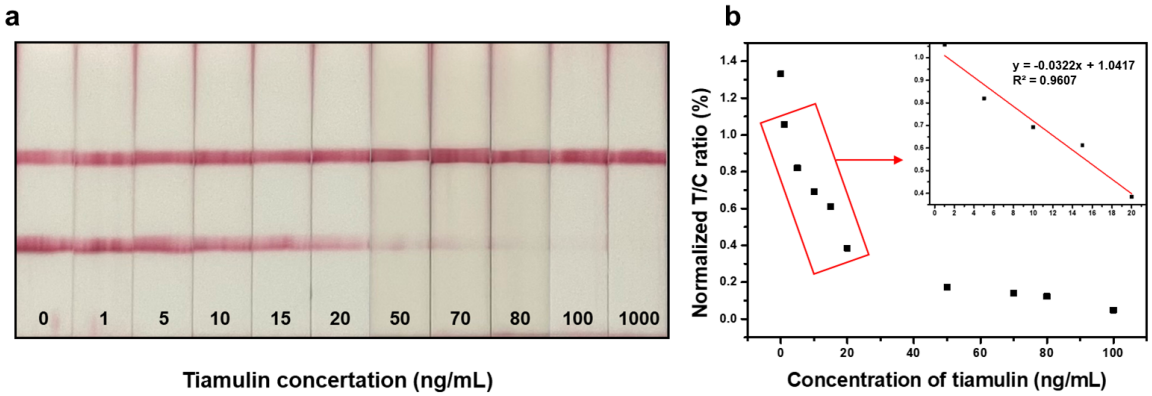

Figure 4. TML determination in standard solutions. (a) Image of LFIA test strips after addition of various concentrations (0, 1, 5, 10, 15, 20, 50, 70, 80, 100, and 1000 ng/mL) of TML. (b) Relationship between normalized T/C ratio and TML concentration. The T/C ratio was calculated by dividing test line intensity by control line intensity. The control line and test line intensity were measured using Image.

value of 100 ng/mL. The vLOD was shown to be 15 ng/mL and obtained a detection range of 0 to 80 ng/mL. The visual results can be displayed within 10 minutes. The image in Fig. 4 (a) was assessed using ImageJ software for further analysis. Fig. 4 (b) demonstrates the relationship between normalized T/C ratio and TML concentration. The intensity of the test and control lines was quantified using the 'Plot Profile' function in ImageJ software. Images were processed by splitting the color channels and selecting the red channel for analysis, followed by background subtraction to improve band contrast. A consistent rectangular area was selected around each line to ensure uniform measurement. Peak intensity values were extracted and used to calculate the signal ratio (T/C) for semi-quantitative interpretation.

As a result, the developed sensor offered a dynamic range of $1-20$ ng/mL with a linear correlation coefficient of $R^2 = 0.9607$. The optimized LFIA test strips accomplished great sensitivity with low LOD values.

To evaluate the LFIA strips specificity and selectivity for TML, we tested different interference molecules, including TML structural analogues (VAL and TYL), veterinary antibiotics such as AMP, CPL, and TET, veterinary feed additives like RAC, and creatine. Fig. 5 (a) depicts images of the test results for the cross-reactivity test where we can observe that the test line color only disappeared in samples number 9 (TML) and 10 (Mixture), meaning that the sensor has high specificity for TML only. In Fig. 5 (b), we can clearly see that all other interference molecules showed no difference to the control sample ($\geq 100\%$), which means that the developed sensor possessed admirable specificity for TML only.

3.4 Determination of TML in spiked milk and egg samples

As the goal of our sensor is the detection of TML in complex matrices, we evaluated its performance in both egg and milk samples. Spiked sample solutions were prepared by mixing real sample and loading buffer at a 1:1 ratio. The milk sample, purchased from a local market, was tested directly without pretreatment to maintain rapid and simple test procedures (Fig. 6 (a)). Milk samples were spiked with different concentrations of TML (0, 5, 15, 80, and 100 ng/mL), and results were analyzed after 10 minutes (Fig. 6 (c)). The detection of TML in milk samples yielded a cut-off value

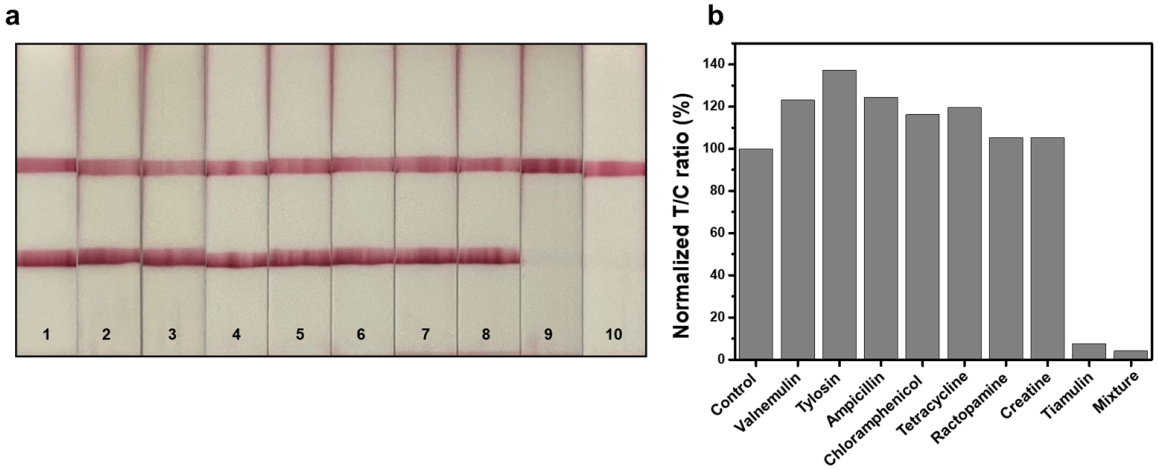

Figure 5. Specificity test of TML and interference molecules at a concentration of 100 ng/mL. (a) Images of the LFIA strips with TML and interference molecules. 1: control, 2: VAL, 3: TYL, 4: AMP, 5: CPL, 6: TET, 7: RAC, 8: Creatin, 9: TML, 10: mixture of VAL + TYL + AMP + CPL + TET + RAC + Creatin + TML. (b) The normalized T/C ratio of LFIA strips produced by the ImageJ program.

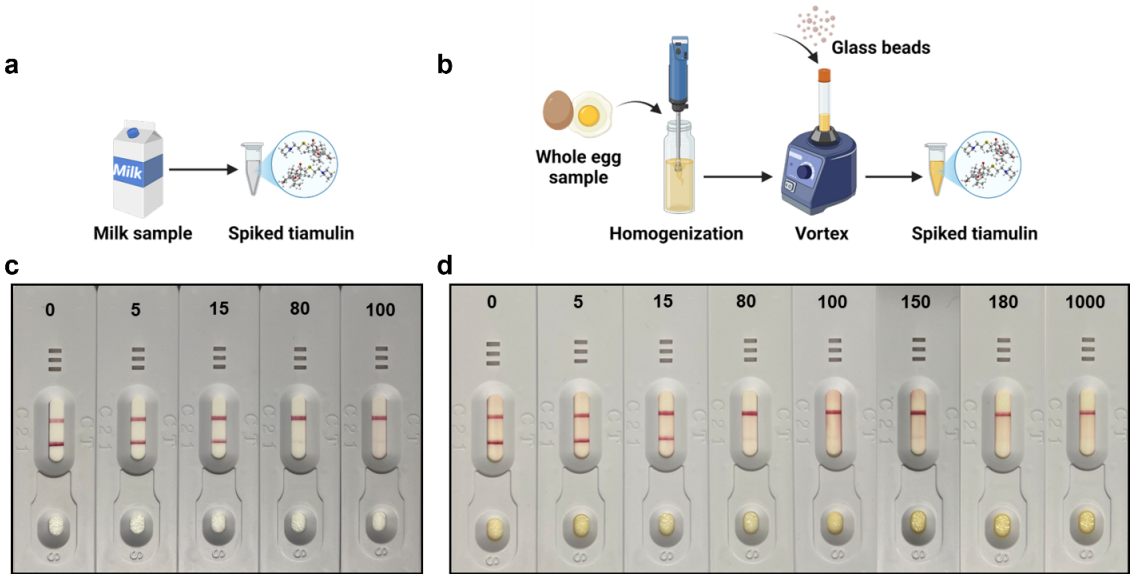

Figure 6. Determination of TML in milk and egg samples. (a) Sample preparation of milk. (b) Sample preparation of egg. (c) LFIA strips images for TML detection in egg samples containing TML at 0, 5, 15, 80, and 100 ng/mL. (d) LFIA strips images for TML detection in egg samples containing TML at concentrations of 0, 5, 15, 80, 100, 150, or 180, 1000 ng/mL.

of 100 ng/mL with a vLOD of 15 ng/mL. Spike–recovery analysis in milk confirmed that quantification was reliable from 15 ng/mL upward, with recoveries of 130.55% (RSD 4.91%) at 15 ng/mL and 95.98% (RSD 2.89%) at 50 ng/mL (Table 1). However, the 5 ng/mL spike in milk failed to meet accuracy and precision criteria, indicating that this level is below the LOQ under pretreatment-free conditions. The reduced performance at low concentrations in milk is likely attributable to matrix interferences, including fat, casein micelles, and lactose, which may elevate background signals, hinder antigen–antibody interactions, and disrupt uniform flow along the strip.

Egg samples were prepared by blending whole egg with a high-speed mixer, then adding beads and vertexing until homogeneous, as illustrated in Fig. 6 (b). The homogenate was spiked with TML at concentrations of 0, 5, 15, 80, 100, 150, 180, and 1000 ng/mL without additional pretreatment. Testing in egg showed a vLOD of 15 ng/mL and a cut-off value of 180 ng/mL (Fig. 6 (d)). In spike–recovery analysis, egg samples achieved acceptable accuracy and precision at all tested levels, with recoveries of 93.62% (RSD 6.99%) at 5 ng/mL, 70.09% (RSD 8.39%) at 15 ng/mL, and 96.34% (RSD 11.73%) at 50 ng/mL. These results indicate that, while both matrices can be analyzed without pretreatment, the LOQ is matrix-specific: 5 ng/mL is quantifiable in egg but not in milk. Overall, the proposed LFIA shows strong tolerance to complex matrices and provides sensitive detection of TML in line with positive list system guidelines, offering the added benefit of rapid and simple field applicability. Given that the system requires no pretreatment, the recoveries achieved are considered highly satisfactory.

To facilitate performance evaluation, a comparison table has been included summarizing the analytical characteristics of different reported methods for TML detection (Table 2). Compared to the two previously reported LFIAs for TML detection, which required complex sample pretreatment, our method offers several key advantages. Specifically, it enables direct testing of milk and egg without any extrac-

Table 1. The spiked recoveries of TML in milk and egg measured by the developed LFIA.

Real matrices	Spiked concentration (ng/mL)	Measured concentration (ng/mL)	Recovery (%)	RSD* (%)
Milk	0	ND[a]	NC[b]	NC
	5[c]	ND	NC	NC
	15	19.58 ± 0.96	130.55	4.91
	50	47.99 ± 1.39	95.98	2.89
Egg	0	ND	NC	NC
	5	4.68 ± 0.33	93.62	6.99
	15	10.51 ± 0.88	70.09	8.39
	50	48.17 ± 5.65	96.34	11.73

*Values are means ± standard deviations (n = 3), a: not detectable, b: not calculated, c: 5 ng/mL is below the method LOQ for milk.

Table 2. Comparison of different methods for the detection of TML.

Technique	Real sample	Pre-treatment time (min)	Detection limit	Recovery/ Precision	Advantages	Disadvantages	Ref.
HPLC	Chicken, pork	∼ 60	LOD: 0.025 µg/mL	84.3% – 105.9% RSD < 8.3%	Good accuracy	Lower sensitivity compared to other chromatography techniques, complex sample preparation, require professional personnel, long analysis time	[31]
UHPLC MS/MS	Sow milk, Piglet serum	∼ 30	LOQ: 1 ng/mL	94% – 107% RSD ≤ 13.4%	High sensitivity, low LOQ, good for biological matrices	Expensive instrumentation, complex sample preparation, require professional personnel, long analysis time	[1]
LC MS/MS	Medicated Feed	∼ 30 – 60	LOD: 4.09 µg/mL LOQ: 6.53 µg/mL	84.5% – 96.3% precision repeatability < 14%, reproducibility < 24%	Multi residue detection capability	Precision range broader, low sensitivity, expensive instrumentation, complex sample preparation, require professional personnel, long analysis time	[6]
LC MS/MS	Muscle, liver, eggs	∼ 60	LOD: 8 ng/mL LOQ: 25 ng/mL	79.6% – 84.2% RSD 6.65% – 11.06%	Good sensitivity	Complex sample extraction, expensive instrumentation, require professional personnel, long analysis time	[4]
Electrochemical immunosensor	Egg, pork, pork liver	∼ 40 – 70	LOD: 0.003 ng/mL	82.8 – 112% RSD 3.55% – 7.31%	Ultra-low LOD, label-free, good accuracy, high reproducibility	Electrode modification required with multiple steps, require professional personnel	[32]
Electrochemical immunosensor	Pork, pork liver	∼ 40	LOD: 0.04 ng/mL	91.3% – 100.3% RSD 5.2% – 17.0%	Sensitive, broad dynamic range, good stability	Electrode modification required with multiple steps, require professional personnel	[8]
Lateral flow immunoassay	Chicken	∼ 20	Cut-off: 5 ng/mL	–	Portable, rapid analysis	Wet method, high antibody concentration required, complicated pretreatment steps	[17]
Lateral flow immunoassay	Porcine liver	∼ 40	LOD: 0.29 ng/g Cut-off: 25 ng/g	80.6% – 102% RSD < 10%	Portable, rapid analysis, good sensitivity	Complicated pretreatment steps, simultaneous detection using a single monoclonal antibody compromise sensitivity and specificity, low antibody specificity	[18]
Lateral flow immunoassay	Egg, milk	No pretreatment	VLOD: 15 ng/mL Cut-off: 180, 100 ng/mL	70% – 130% RSD > 12%	Pretreatment-free, high specificity of antibody, high tolerance for sample matrix, portable, rapid analysis	Need integration with LFIA reader for more accurate quantitative detection	This work

tion or cleanup steps, employs highly specific antibodies, and exhibits strong resistance to matrix interference. These improvements enhance the practical usability of the assay for field-level residue screening and align more closely with real-world monitoring needs in food safety. In addition to LFIAs, a limited number of studies have explored alternative portable approaches for the on-site detection of TML, most notably electrochemical immunosensors. While such sensors can provide enhanced sensitivity and are amenable to miniaturization, they often require more complex instrumentation and signal interpretation, which may limit their practicality in field settings compared to visually readable lateral flow assays. Furthermore, validation of these electrochemical platforms across diverse sample matrices remains limited. In summary, the proposed LFIA addresses key limitations of existing TML detection methods by combining pretreatment-free operation, high antibody specificity, and strong matrix tolerance, thereby offering a field-deployable solution aligned with current food safety monitoring requirements.

4. Conclusion

In this study, we fabricated LFIA system using AuNPs ($\approx 1.34 \times 10^{12}$ nanoparticles/mL) conjugated with highly specific TML-Ab for simple, rapid, and pretreatment-free qualitative and semi-quantitative detection of TML. The assay demonstrated a vLOD of 15 ng/mL for both egg and milk samples, with clear cut-off values of 100 ng/mL for milk and 180 ng/mL for egg. The RSD values were below 12%, showing high recoveries in both milk and egg matrices. The primary goal of this work was to establish a strategy for TML determination in milk and egg that shortens sample collection times, eliminates labor-intensive pretreatment steps, and improves production efficiency. Compared with previously reported chromatographic, electrochemical, and LFIA-based methods, our approach offers distinct advantages by eliminating complex pretreatment procedures, utilizing a highly specific antibody to ensure accurate detection without cross-reactivity, and achieving good detection limits within 10 minutes of analysis while meeting the regulatory requirements of Korea's positive list system. The developed LFIA exhibited high tolerance to matrix effects, enabling direct analysis without loss of performance in complex food matrices. These attributes make the proposed sensor a promising, cost-effective, and user-friendly tool for the on-site monitoring of veterinary drug residues in animal-derived products, supporting routine food safety surveillance. In future work, we aim to integrate the system with an LFIA reader for improved quantitative capability and further enhance its matrix tolerance to broaden its applicability to more challenging sample types.

Acknowledgment

This work was carried out with the funding of the "Co-operative Research Program for Agriculture Science and Technology Development (Project No. PJ014238042022)" Rural Development Administration, Republic of Korea and ⌜Development of Field Technology for Responding to Illegal drugs⌟ Program through the Korea Institutes of Police Technology(KIPoT) funded by the Korean National Police Agency & Korea Customs Service. (RS-2024-00406234)

Authors Contribution

MA: Methodology, data curation, validation, investigation, and writing–original draft. SS: Formal analysis, and methodology. SH and HK: Methodology. DHK, MHO, and YSH: Conceptualization, project administration, investigation, and writing–review and editing.

Availability of data and materials

All data generated or analysed during this study are included in this published article and its supplementary information files.

Conflict of interests

The authors declare that they have no known competing financial interests or personal relationships that could have appeared to influence the work reported in this paper.

References

[1] P. Cybulski, A. Gajda, M. Bilecka, and A. Jabłonski. "Determination of Tiamulin Concentration in Sow Milk and in Sera of Suckling Piglets". *Molecules*, **28**(6940), 2023.

[2] M. D. Borak, L. Sarc, D. G. Mugerli, B. Antolic, and M. Brvar. "Occupational inhalation poisoning with the veterinary antibiotic tiamulin". *Clin. Toxicol.*, **58**(287), 2020.

[3] E. Pankowska, O. Kończak, P. Żakowicz, T. Wojciechowicz, M. Gogulski, and L. Radko. "Protective Action of Cannabidiol on Tiamulin Toxicity in Humans—In Vitro Study". *Int. J. Mol. Sci.*, **25**:13542, 2024.

[4] J. Oszmianski, S. Lachowicz, W. Wi´sniewska, V. C. Ciuca, C. O. Rusanescu, and V. V. Safta. "Analysis of Transfer of Tiamulin to Animal Tissue after Oral Administration: An Important Factor for Ensuring Food Safety and Environmental Protection". *Pharmaceuticals*, **16**:387, 2023.

[5] *Ministry of Food and Drug Safety*. URL https://www.mfds.go.kr/eng/index.do.

[6] E. Patyra, C. Nebot, R. E. Gavilán, A. Cepeda, and K. Kwiatek. "Development and validation of an LC-MS/MS method for the quantification of tiamulin, trimethoprim, tylosin, sulfadiazine and sulfamethazine in medicated feed". *Food Addit. Contam.: Part A.*, **35**: 882, 2018.

[7] F. Sun et al. "Comprehensive analysis of tiamulin metabolites in various species of farm animals using ultra-high-performance liquid chromatography coupled to quadrupole/time-of-flight". *J. Agric. Food Chem.*, **65**:199, 2017.

[8] X. Yo et al. "A novel electrochemical immunosensor for the sensitive detection of tiamulin based on staphylococcal protein A and silver nanoparticle-graphene oxide nanocomposites". *Bioelectrochemistry*, **141**:107877, 2021.

[9] J. Zhou, X. Zhang, W. Qian, Q. Yang, Y. Qi, Y. Chen, and A. Wang. "Quantum dots-based fluorescence immunoassay for detection of tiamulin in pork". *J. Food Saf.*, **41**:e12930, 2021.

[10] L. Li, J. Y. Yang, Y. Wang, Z. Zhang, T. T. Yuan, Y. M. Xiao, Z. L. Xu, and Y. D. Shen. "Development of a Chemiluminescence Enzyme Immunoassay Method for Detection of Tiamulin Residues in Eggs". *J. Instrum. Anal.*, **41**:115, 2022.

[11] M. F. Lanjwani, N. Altunay, and M. Tuzen. "Preparation of fatty acid-based ternary deep eutectic solvents: Application for determination of tetracycline residue in water, honey and milk samples by using vortex-assisted microextraction". *Food Chem.*, **400**:134085, 2023.

[12] M. Nemati, M. R. Afshar Mogaddam, M. A. Farazajdeh, M. Tuzen, and J. Khandaghi. "In-situ formation/decomposition of deep eutectic solvent during solidification of floating organic droplet-liquid-liquid microextraction method for the extraction of some antibiotics from honey prior to high performance liquid chromatography-tandem mass spectrometry". *J. Chromatogr. A*, **1660**:462653, 2021.

[13] A. C. Mirica, D. Stan, I. C. Chelcea, C. M. Mihailescu, A. Ofiteru, and L. A. Bocancia-Mateescu. "Latest Trends in Lateral Flow Immunoassay (LFIA) Detection Labels and Conjugation Process". *Front Bioeng. Biotechnol.*, **10**:922772, 2022.

[14] K. H. Kim et al. "Low-Powered pH-Stable Nano-electrokinetically Enhanced Lateral Flow Assay for COVID-19 Antigen Test". *Biochip J.*, **17**:340, 2023.

[15] F. Zhao, K. Wangpimool, and J. C. Kim. "Near-infrared and Thermo-sensitive Liposomes Incorporating Thiolated-carboxymethyl Cellulose-capped Gold Nanoparticles and Poly(N-isopropylacrylamide)". *Biotechnol. Bioprocess Eng.*, **28**:589, 2023.

[16] Q. Dai, S. Tang, and C. Dai. "Recent Advances in Pretreatment Methods and Detection Techniques for Veterinary Drug Residues in Animal-Derived Foods". *Metabolites*, **15**:233, 2025.

[17] X. Lei, S. Song, H. Tao, L. Liu, Q. Zheng, C. Xu, and H. Kuang. "Development of Indirect Competitive Enzyme-Linked Immunosorbent and Immunochromatographic Strip Assays for Tiamulin Detection in Chicken". *ACS Omega.*, **3**:3581, 2018.

[18] G. Na, X. Hu, Y. Sun, S. Kwee, G. Xing, Y. Xing, and G. Zhang. "A highly sensitive monoclonal antibody-based paper sensor for simultaneously detecting valnemulin and tiamulin in porcine liver". *J. Food Sci.*, **85**:1681, 2020.

[19] J. Dong, P. L. Carpinone, G. Pyrgiotakis, P. Demokritou, and B. M. Moudgil. "Synthesis of Precision Gold Nanoparticles Using Turkevich Method". *Kona*, **37**:224, 2020.

[20] M. Alhammadi, S. Aliya, R. Umapathi, M. H. Oh, and Y. S. Huh. "A simultaneous qualitative and quantitative lateral flow immunoassay for on-site and rapid detection of streptomycin in pig blood serum and urine". *Microchem. J.*, **195**:109427, 2023.

[21] Y. Moon, H. H. Cho, H. Moon, H. Song, J. C. Ro, J. H. Lee, and J. Lee. "Simultaneous Triplex Detection in a Single-Test-Line Lateral Flow Immunoassay Utilizing Distinct Nanoparticle Colorimetry". *Biochip J.*, **18**:247, 2024.

[22] G. A. Posthuma-Trumpie, J. Korf, and A. Van Amerongen. "Lateral flow (immuno)assay: Its strengths, weaknesses, opportunities and threats. A literature survey". *Anal. Bioanal. Chem.*, **393**:569, 2009.

[23] V. P. Shah et al. "Bioanalytical method validation - A revisit with a decade of progress". *Pharm. Res.*, **17**:1551, 2000.

[24] H. Tyagi, A. Kushwaha, A. Kumar, and M. Aslam. "A Facile pH Controlled Citrate-Based Reduction Method for Gold Nanoparticle Synthesis at Room Temperature". *Nanoscale. Res. Lett.*, **11**:1, 2016.

[25] D. Philip. "Green synthesis of gold and silver nanoparticles using Hibiscus rosa sinensis". *Physica E Low Dimens. Syst. Nanostruct.*, **42**:1417, 2010.

[26] J. O. Tam, H. de Puig, C. wan Yen, I. Bosch, J. Gómez-Márquez, C. Clavet, K. Hamad-Schifferli, and L. Gehrke. "A Comparison of Nanoparticle-Antibody Conjugation Strategies in Sandwich Immunoassays". *J. Immunoassay Immunochem.*, **38**:355, 2016.

[27] J. P. Oliveira, A. R. Prado, W. J. Keijok, P. W. P. Antunes, E. R. Yapuchura, and M. C. C. Guimaraes. "Impact of conjugation strategies for targeting of antibodies in gold nanoparticles for ultrasensitive detection of 17β-estradiol". *Sci. Rep.*, **9**:1, 2019.

[28] O. D. Hendrickson, N. A. Byzova, E. A. Zvereva, A. V. Zherdev, and B. B. Dzantiev. "Sensitive lateral flow immunoassay of an antibiotic neomycin in foodstuffs". *J. Food Sci. Technol.*, **58**:292, 2021.

[29] Y. Wang, B. Ma, M. Liu, E. Chen, Y. Xu, and M. Zhang. "Europium Fluorescent Nanoparticles-Based Multiplex Lateral Flow Immunoassay for Simultaneous Detection of Three Antibiotic Families Residue". *Front. Chem.*, **9**:793355, 2021.

[30] M. Alhammadi, J. Yoo, S. Sonwal, S. Y. Park, R. Umapathi, M. H. Oh, and Y. S. Huh. "A highly sensitive lateral flow immunoassay for the rapid and on-site detection of enrofloxacin in milk". *, Front. Nutr.*, **9**:1036826, 2022.

[31] H.-C. Chen, S.-H. Cheng, Y.-H. Tsai, D.-F. Hwang, H.-C. Chen, S.-H. Cheng, Y.-H. Tsai, and A.D.-F. Hwang. "Determination of tiamulin residue in pork and chicken by solid phase extraction and HPLC". *J. Food Drug Anal.*, **14**:2, 2020.

[32] A. Wang et al. "Development of a label free electrochemical sensor based on a sensitive monoclonal antibody for the detection of tiamulin". *Food Chem.*, **366**:130573, 2022.

Supplementary Table 1. Specifications of TML antibody used in this study.

Item	Description
Product name	Mouse Anti-Tiamulin Monoclonal Antibody, Clone TML
Catalog number	CABT-L3067
Supplier	Creative Diagnostics, Shirley, NY, USA
Host species	Mouse
Isotype	IgG
Clone	TML
Immunogen	Tiamulin conjugated with a carrier protein
Conjugation	Unconjugated
Purification method	Purified from mouse ascites
Applications	ELISA, LFIA
Format	Liquid
Buffer	PBS (no preservative)
Concentration	6 mg/mL
Batch/Lot number	JW07B121
Storage conditions	−20 °C for long-term storage
Intended use	For research use only

Supplementary Table 2. Nitrocellulose membrane specifications.

Item	Specification
Backing	100 µm polyester
Membrane thickness	95–135 µm
Wicking rate	70 – 100 s/4 cm
Pore size	15 µm
Width	25 mm

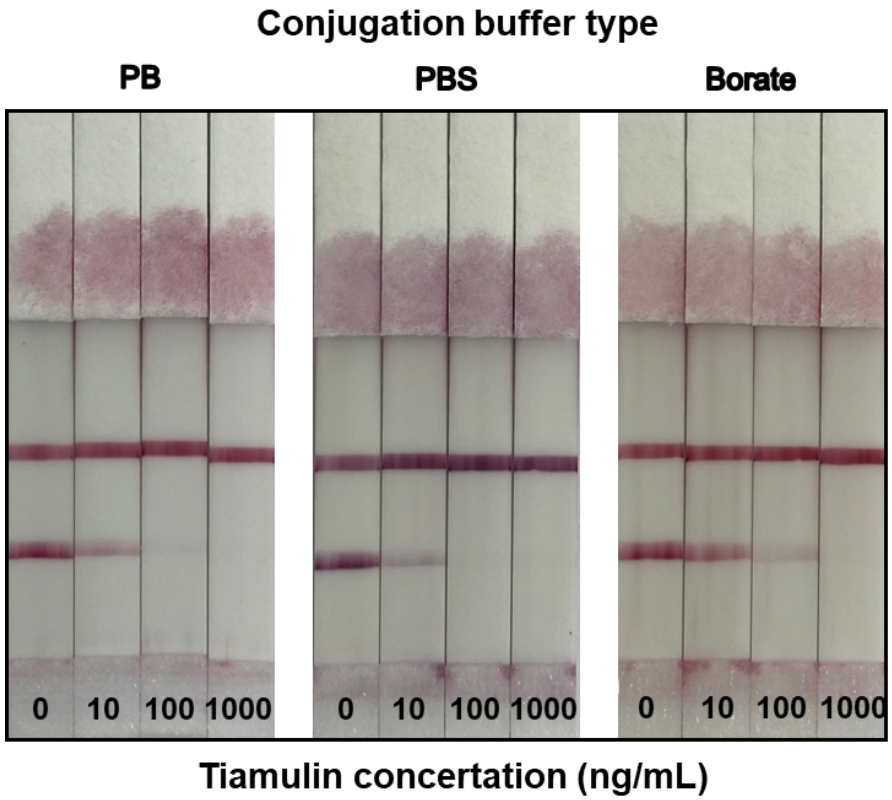

Supplementary Figure 1. Optimization of LFIA strip for the detection of TML. Effect of the various types of blocking buffers on LFIA strips. The TML sample concentrations are 0, 10, 100 and 1000 ng/mL.

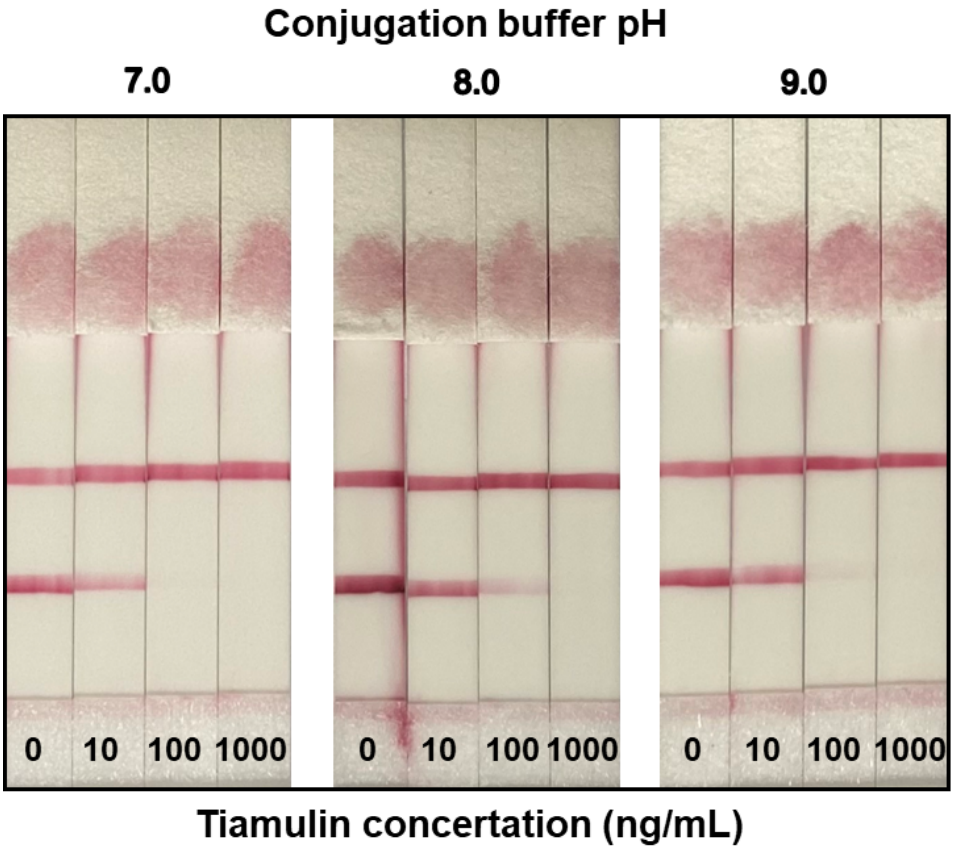

Supplementary Figure 2. Optimization of LFIA strip for the detection of TML. Effect of the various pH values (7, 8, 9) of 10 mM PB on LFIA strips. The TML sample concentrations are 0, 10, 100 and 1000 ng/mL.

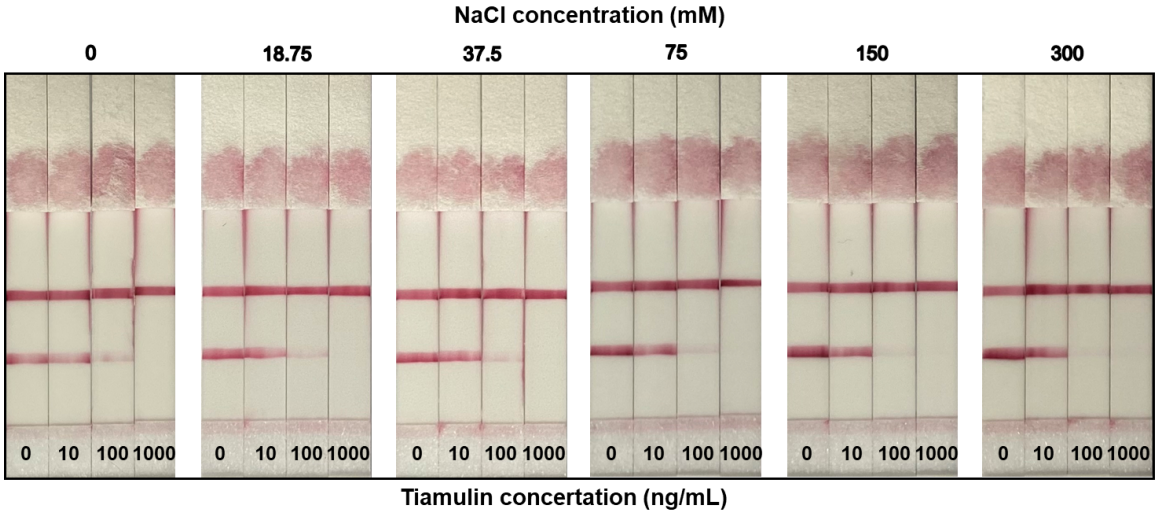

Supplementary Figure 3. Optimization results of NaCl at different concentrations (0, 18.75, 37.5, 75, 150, and 300 mM) on LFIA test strips. The TML sample concentrations are 0, 10, 100 and 1000 ng/mL.

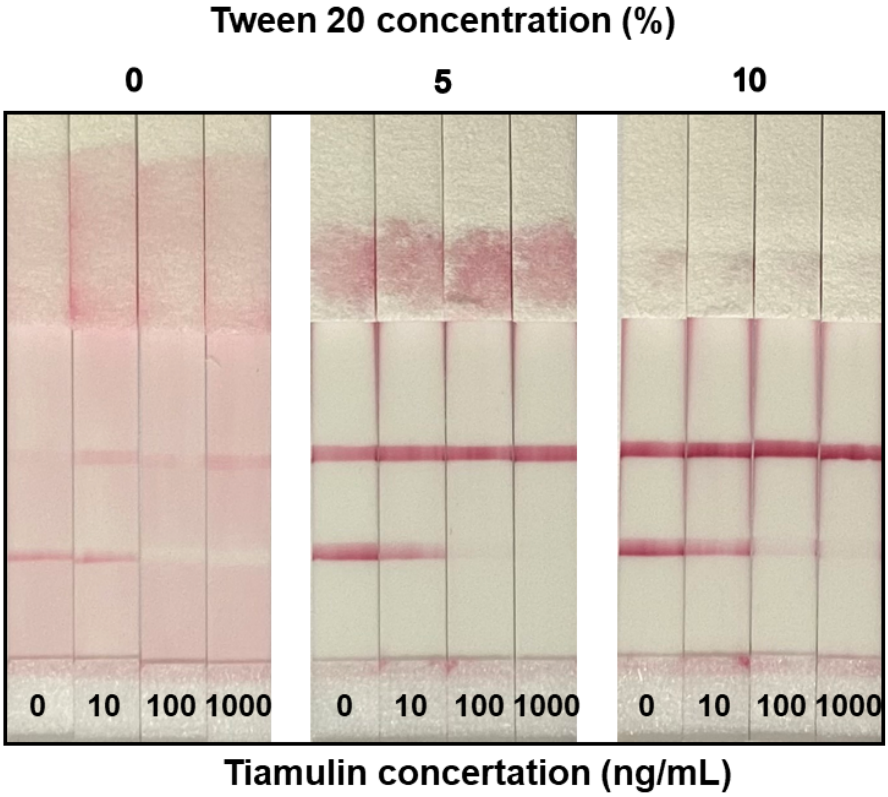

Supplementary Figure 4. Optimization results of tween 20 at different concentrations (0, 5, and 10%) on LFIA test strips. The TML sample concentrations are 0, 10, 100 and 1000 ng/mL.